

Lattice inversion for interionic pair potentials

Shuo Zhang^{a)}

Department of Physics, Tsinghua University, 100084, Beijing, China and National Key Laboratory for Material Simulation and Design, 100083 Beijing, China

Nan-xian Chen

Department of Physics, Tsinghua University, 100084 Beijing, China, Institute for Applied Physics, University of Science and Technology Beijing, 100083 Beijing, China and National Key Laboratory for Materials Simulation and Design, 100083 Beijing, China

(Received 1 July 2002; accepted 10 December 2002)

The *ab initio* total energies of alkali chloride crystals in B1 (rock salt), B2 (CsCl-type), B3 (zinc blende) and P4/mmm structures are calculated by ultrasoft pseudopotential method in this paper. Based on the different combinations of these total energies, the effective charges on ions are determined for long-range Coulomb interaction, and the short-range potential curves are obtained by the lattice inversion method. As the test for the quality of potentials, the static properties of AgCl in the rock salt phase are calculated. The results are in good agreement with the experimental data. And the calculated lattice energies for AgCl in wurtzite, CuAu, NiAs, and litharge structures are consistent with the predictions of pseudopotential calculations. In terms of the molecular dynamics simulations, the temperature dependences of volume, bulk modulus, and elastic constants are also investigated from room temperature to 800 K, the results are in good agreement with the experimental values. This indicates that the new interionic potentials are valid over a wide range of interionic separations and coordination numbers. © 2003 American Institute of Physics.
[DOI: 10.1063/1.1542876]

I. INTRODUCTION

The atomistic simulations on structures and properties of ionic crystals have been given great interest for their typical ionic bonded structures and wide applications.¹⁻⁸ One of the key problems for the atomistic simulations is how to determine the interionic potentials. In most of the previous work,^{2,3,5,9-15} the interionic potentials were started from the selection of interionic potential function forms with adjustable parameters, and then the potential parameters were obtained by fitting to the experimental data or calculation results, such as lattice parameters, lattice energy, phonon frequencies, elastic, and dielectric properties. The interionic potential models often consist of the long-range and short-range terms; the former is usually described as the Coulomb interaction with formal or M \ddot{u} lliken charges, and the latter is overlap repulsive interaction with different adjustable parameters. These potentials have played a significant role in previous simulations, especially for the ionic materials with lots of experimental data.^{2,3,7} However, for the ionic solids whose properties are hard to obtain, the parameters of interionic potentials have to be derived from calculations, such as the *ab initio* calculations. On this occasion, if the multiple-parameter fitting method is still used, the advantages of *ab initio* calculations may not totally be exhibited. Since the adjustable parameters are involved, the uncertain and arbitrary parameters are often involved by providing several sets of potential parameters,^{3,15} and it is hard to determine which set of potentials is the most appropriate.

One of the effective solutions for the uncertainty of multiple-parameter fittings may be the lattice inversion method, which was first presented to determine the pairwise potentials from the *ab initio* calculated or experimentally measured cohesive energy by Carlsson, Gelatt, and Ehrenreich (CGE),¹⁶ and then Chen used the Mobius-inversion formula in number theory not only to obtain the pair potentials for the pure metals,¹⁷ but also for the intermetallic compounds^{18,19} with faster convergence²⁰ than the CGE method. However, so far the lattice inversion has not been applied for ionic crystals because the ionic charge density distribution is obviously different from that of a free atom. From the viewpoint of lattice inversion, let us show the comparison of the interatomic potentials in binary alloy Fe₃Al¹⁸ with the interionic potentials in ionic crystal NaCl. In the first case, there are three distinct pair interaction functions: $\phi_{\text{Fe-Fe}}$, $\phi_{\text{Al-Fe}}$, and $\phi_{\text{Al-Al}}$, in which $\phi_{\text{Fe-Fe}}$ and $\phi_{\text{Al-Al}}$ can be obtained by lattice inversion techniques from *ab initio* cohesive energies of iron and aluminum face-centered-cubic (fcc) lattices, respectively, and then the $\phi_{\text{Al-Fe}}$ can easily be determined from Fe₃Al cohesive energy. The reason is that there is a very slight difference between the charge densities of fcc pure metals and the binary alloy. But in the second case, it is also needed to determine three different interaction functions: $\phi_{\text{Na}^+-\text{Na}^+}$, $\phi_{\text{Cl}^--\text{Cl}^-}$, and $\phi_{\text{Na}^+-\text{Cl}^-}$, whereas $\phi_{\text{Na}^+-\text{Na}^+}$ and $\phi_{\text{Cl}^--\text{Cl}^-}$ cannot be obtained by the same lattice inversion for any ionic crystals constituted only by one kind of like-sign ions. Suppose that each of the interaction potentials described by three parameters have to face the difficulty of how to determine nine parameters only from one NaCl total energy curve.

^{a)}Author to whom correspondence should be addressed. Electronic mail: zhangshuo@mails.tsinghua.edu.cn; Telephone and fax: 86-10-62772783.

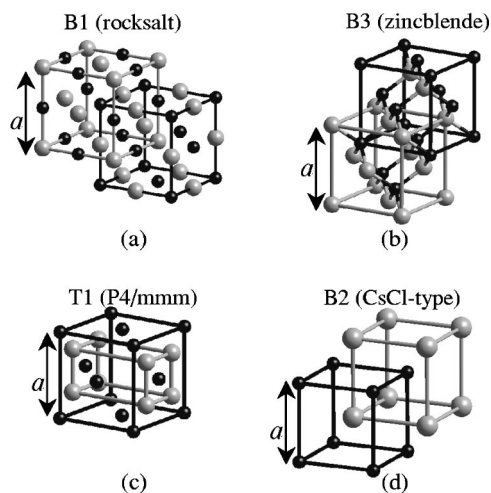


FIG. 1. Virtual structures used for pseudopotential total-energy calculations. The cation and anion are identified by black and gray balls, respectively. (a) (rock salt): fcc cation+fcc anion; (b) B3 (zinc blende): fcc cation+fcc anion; (c) P4/mmm: fcc cation+tetragonal anion; (d) B2 (CsCl-type): sc cation+sc anion.

In order to derive the interionic pair potentials by lattice inversion, we define the partial energy as the sum of only one pair potential that can be obtained. Then in this paper the method of virtual structures is introduced to separate the partial lattice energy from the combination of pseudopotential total-energy curves by taking the alkali chlorides ACl ($A = \text{Li, Na, K, Rb}$) as the prototypical system, which mostly have the rock salt (B1) structures. In terms of the B1 structure, the other three virtual structural models have been built for ACl, as shown in Fig. 1, where the rock salt (B1) and zinc blende (B3) all contain two fcc like-sign ionic sublattices, the structure with P4/mmm symmetry includes one fcc and one tetragonal sublattices, and the B2 (CsCl-type) structure has two identical simple-cubic (sc) sublattices. Based on the description of interionic pair potentials, the interaction between two ions only depends on the interionic separation, and then the interionic pair potentials are assumed as transferable in B1, B2, B3, and P4/mmm structures. Therefore, once the corresponding pseudopotential total energy as a function of lattice constant is obtained for each structure, the three partial lattice energies can be extracted from the total-energy differences between B1 and its virtual structures, respectively. Then the interionic pair potentials can be derived by Chen–Möbius lattice inversion.¹⁷ The details are described in the following text.

II. DERIVATION OF INTERIONIC PAIR POTENTIALS

A. Virtual structural models

For the rock salt-type ACl crystals, the B2, B3, and P4/mmm models have been introduced, as shown in Fig. 1. If the four structures have the identical lattice constant a , then from B1 to B3 only the cation–anion interaction undergoes the change for their identical like-sign ionic sublattices. The total-energy difference per ion between B1 and B3 can be regarded as the partial lattice energy only as the sum of pair potential ϕ_{+-} , and can then be written as

$$\begin{aligned} \Delta E_{+-}(a) &= E_{\text{tot}}^{\text{B1}}(a) - E_{\text{tot}}^{\text{B3}}(a) \\ &= \frac{1}{2} \sum_{i,j,k} \phi_{+-} \\ &\quad \times \left[\sqrt{(i+j-1)^2 + (i+k-1)^2 + (j+k-1)^2} \frac{a}{2} \right] \\ &\quad - \frac{1}{2} \sum_{i,j,k} \phi_{+-} \\ &\quad \times \left[\sqrt{\left(i+j-\frac{1}{2}\right)^2 + \left(i+k-\frac{1}{2}\right)^2 + \left(j+k-\frac{1}{2}\right)^2} \frac{a}{2} \right], \end{aligned} \quad (1)$$

in which the $E_{\text{tot}}^{\text{B1}}(a)$ and $E_{\text{tot}}^{\text{B3}}(a)$ are the pseudopotential total energies per ion of B1- and B3-ACl corresponding to lattice constant a , and i, j , and k indicate the lattice sites of ions.

For B1 and P4/mmm structures, since they have the identical cation sublattice, their total-energy difference should be independent of the cation–cation interaction. With the potential ϕ_{+-} obtained from Eq. (1), the cation–anion interactions $E_{+-}^{\text{B1}}(a)$ and $E_{+-}^{\text{P4/mmm}}(a)$ in B1- and P4/mmm-ACl can be calculated, respectively. Then the anion–anion partial lattice energy per ion can be given as follows:

$$\begin{aligned} \Delta E_{--}(a) &= E_{\text{tot}}^{\text{B1}}(a) - E_{+-}^{\text{B1}}(a) - E_{\text{tot}}^{\text{P4/mmm}}(a) + E_{+-}^{\text{P4/mmm}}(a) \\ &= \frac{1}{4} \sum_{i,j,k \neq 0} \phi_{--} \left[\sqrt{(i+j)^2 + (i+k)^2 + (j+k)^2} \frac{a}{2} \right] \\ &\quad - \frac{1}{4} \sum_{i,j,k \neq 0} \phi_{--} \left[\sqrt{i^2 + 4j^2 + k^2} \frac{a}{2} \right], \end{aligned} \quad (2)$$

in which $E_{\text{tot}}^{\text{P4/mmm}}(a)$ is the pseudopotential total energy of P4/mmm-ACl with lattice constant a , and the ϕ_{--} is the anion–anion pair potential.

Consequently, the anion–anion interaction $E_{--}^{\text{B1}}(a)$ and $E_{--}^{\text{B2}}(a)$ can be separately calculated for B1- and B2-ACl, so the anion–anion partial lattice energy per ion can also be obtained as follows:

$$\begin{aligned} \Delta E_{++}(a) &= E_{\text{tot}}^{\text{B1}}(a) - E_{+-}^{\text{B1}}(a) - E_{--}^{\text{B1}}(a) - E_{\text{tot}}^{\text{B2}}(a) \\ &\quad + E_{+-}^{\text{B2}}(a) + E_{--}^{\text{B2}}(a) \\ &= \frac{1}{4} \sum_{i,j,k \neq 0} \phi_{++} \left[\sqrt{(i+j)^2 + (i+k)^2 + (j+k)^2} \frac{a}{2} \right] \\ &\quad - \frac{1}{4} \sum_{i,j,k \neq 0} \phi_{++} \left[\sqrt{i^2 + j^2 + k^2} a \right], \end{aligned} \quad (3)$$

where $E_{\text{tot}}^{\text{B2}}(a)$ is the pseudopotential total energy per ion in the B2 structure, the $E_{+-}^{\text{B2}}(a)$ is the cation–anion interaction for an average ion in B2-ACl, and ϕ_{++} is the cation–cation pair potential.

TABLE I. The kinetic energy cutoff for plane waves in pseudopotential calculations.

ACI	LiCl	NaCl	KCl	RbCl
E_{cutoff} (eV)	340	410	260	260

B. Pseudopotential total-energy calculations for ACI

In the present work the pseudopotential total energies of ACI crystals are calculated based on the CASTEP (Cambridge Serial Total Energy Package),^{21,22} the pseudopotential plane-wave code developed by MSI. During our calculations, the ultrasoft pseudopotentials for alkali chloride ions are adopted and the GGA-PW91 (General Gradient Approximation) method²³ has been used to cope with the exchange-correlation energy. The k -mesh points over the Brillouin zone are generated with parameters $4 \times 4 \times 4$ for the biggest reciprocal space and $1 \times 1 \times 1$ for the smallest one by the Monkhorst–Pack scheme²⁴ corresponding to the lattice constant a . The energy tolerance for self-consistent-field (SCF) convergence is 2×10^{-6} eV/atom. The kinetic energy cutoff for a plane wave basis set in different ACI crystals is shown in Table I. Then the calculated total energy as a function of lattice constant a is shown in Fig. 2.

C. Lattice inversion for interionic pair potentials

1. Chen–Möbius lattice inversion

Based on the Chen–Möbius lattice inversion,^{17,18} the crystal lattice energy $E(x)$ for each atom can be expressed as a sum of pair potential $\phi(x)$, such that

$$E(x) = \frac{1}{2} \sum_{R_i \neq 0} \phi(R_i) = \frac{1}{2} \sum_{n=1}^{\infty} r_0(n) \phi(b_0(n)x), \quad (4)$$

where x is the nearest neighbor distance, R_i is the lattice vector of the i th atom, $b_0(n)x$ is the n th-neighbor distance, and $r_0(n)$ is the n th coordination number. We extended the series, $\{b_0(n)\}$, into a multiplicative semigroup such that, for any two integers m and n , there always exists an integer k , such that

$$b(k) = b(m)b(n). \quad (5)$$

Equation (4) can be rewritten as

$$E(x) = \frac{1}{2} \sum_{n=1}^{\infty} r(n) \phi(b(n)x), \quad (6)$$

in which

$$r(n) = \begin{cases} r_0(b_0^{-1}[b(n)]) & \text{if } b(n) \in \{b_0(n)\}, \\ 0 & \text{if } b(n) \notin \{b_0(n)\}. \end{cases} \quad (7)$$

Thus, the pair potential, $\phi(x)$, can be written as

$$\phi(x) = 2 \sum_{n=1}^{\infty} I(n) E(b(n)x), \quad (8)$$

where $I(n)$, the inversion coefficient, can be uniquely determined from the crystal structure as

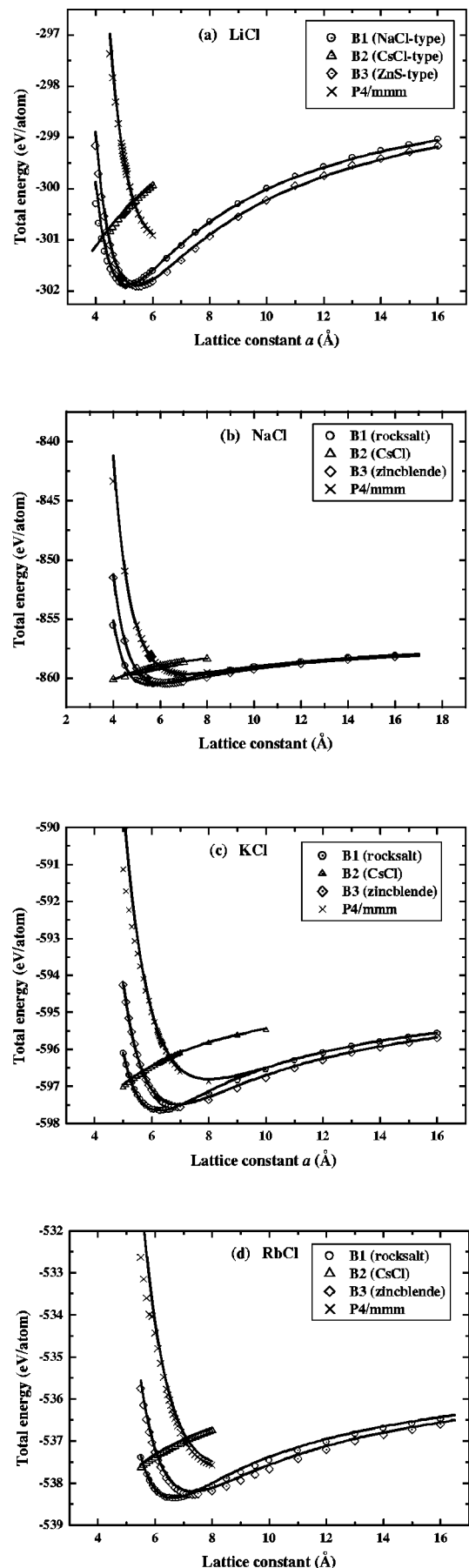


FIG. 2. Total energies vs lattice constant a in different virtual structures from *ab initio* pseudopotential calculations.

$$\sum_{b(n)|b(k)} I(n)r \left(b^{-1} \left[\frac{b(k)}{b(n)} \right] \right) = \delta_{k1}. \quad (9)$$

Note that this inversion coefficient $I(n)$ is only structure dependent; then the coefficients $I_{+-}(n)$, $b_{+-}(n)$, $I_{--}(n)$, $b_{--}(n)$, $I_{++}(n)$, and $b_{++}(n)$ can be obtained from Eqs. (1), (2), and (3), respectively.

2. Long-range Coulomb interaction

In general, each pair potential can be derived in terms of the partial lattice energy and corresponding inversion coefficients. However, for ionic crystal, the long-range Coulomb interaction is the dominant part and has the slow convergence with the interionic spacing r (which is proportional to $1/r$), and this is very difficult for the lattice inversion method. The reason is that the lattice inversion demands the pair potentials decay more rapidly with distance r than the potential proportional to $1/(4\pi r^2 N_\rho)$ because the number of interactions increases as $4\pi r^2 N_\rho$, where N_ρ is the particle number density. A sufficient condition for convergence is $|E(r)| < A/r^3$ for some $A > 0$ in three dimensions,¹⁶ this condition is not obviously satisfied by the Coulomb energy. Hence, we have to decompose the components of the lattice energy into two classes: long-range Coulomb part and short-range potentials. The Coulomb term is treated by Madelung method²⁵ or Ewald summation techniques²⁶ with the fixed ionic charges. And the short-range potential parameters are obtained by Chen's lattice inversion in terms of the coefficients $I_{+-}(n)$, $b_{+-}(n)$, $I_{--}(n)$, $b_{--}(n)$, $I_{++}(n)$, and $b_{++}(n)$.

In order to take account of the Coulomb term, the fixed charges on ions were used in our scheme. In the previous work,^{11,13,14} the formal charges or M\"ulliken charges were often used. Here the fixed charges on ions are determined by the pseudopotential total energy difference between B1- and B3-ACI at a larger lattice constant. The detail can be described as follows: First the pseudopotential total-energy calculations are extended to the lattice constant $a = 16.0 \text{ \AA}$ for B1- and B3-ACI. Since the Coulomb interaction has the slow convergence, the ionic interaction can be approximately devoted only by the Coulomb potential at larger interionic spacing. Then when the lattice constant $a \geq 10.0 \text{ \AA}$, the lattice energies are approximately regarded as only the sum of Coulomb potential, so the total-energy difference between B1- and B3-ACI is

$$E_{\text{tot}}^{\text{B1}}(a) - E_{\text{tot}}^{\text{B3}}(a) = E_{\text{Coul}}^{\text{B1}}(a) - E_{\text{Coul}}^{\text{B3}}(a), \quad (10)$$

where the Coulomb interactions, $E_{\text{Coul}}^{\text{B1}}(a)$ and $E_{\text{Coul}}^{\text{B3}}(a)$ in B1- and B3-ACI, can be calculated via the Madelung constants²⁵ of B1 and B3 structures. Therefore, the fixed ionic charges can finally be determined by fitting the total-energy difference between B1- and B3-ACI at a larger lattice constant. The results are listed in Table II for the four ACI crystals. Once the fixed ionic charges have been calculated, the long-range Coulomb interactions can be determined by Madelung method or Ewald summation techniques.^{25,26}

TABLE II. The effective charges obtained by fitting to the total-energy difference between B1- and B3-ACI.

ACI	LiCl	NaCl	KCl	RbCl
$ q_+ = q_- $	1.013 e	1.005 e	1.000 e	0.991 e

3. Lattice inversion for short-range potential

With the fixed ionic charges, the Coulomb terms can be extracted from the partial lattice energies, and the short-range partial lattice energies can also be obtained for each pair potential. Then with the above inversion coefficients, $I_{+-}(n)$, $b_{+-}(n)$, $I_{--}(n)$, $b_{--}(n)$, $I_{++}(n)$, and $b_{++}(n)$, the ϕ_{+-}^{SR} , ϕ_{--}^{SR} , and ϕ_{++}^{SR} short-range pair potential curves can be inverted from different short-range partial lattice energies, respectively. According to the shapes of curves, the suitable potential function forms are selected to fit the potential curves. Particular in this work, the short-range potential function forms are expressed as Morse type,

$$\phi^{\text{SR}}(r) = D \left\{ \exp \left[-\gamma \left(\frac{r}{R} - 1 \right) \right] - 2 \left[-\frac{\gamma}{2} \left(\frac{r}{R} - 1 \right) \right] \right\}, \quad (11)$$

and a repulsive exponential (Rep.-Exp.) function,

$$\phi^{\text{SR}}(r) = D \exp \left[-\gamma \left(\frac{r}{R} - 1 \right) \right]. \quad (12)$$

The short-range potential parameters are listed in Table III.

III. TEST FOR THE INTERIONIC PAIR POTENTIALS

A. Lattice energies in different structures

As the test for the validity, the present interionic potentials should first correctly reproduce the total energies of B1-, B2-, B3-, and P4/mmm ACI. With the potential parameters in Table III, the lattice energies of B1-, B2-, B3-, and P4/mmm ACI were calculated, and the corresponding isolated-ion energies (the difference between lattice energy and total energy) were also obtained and listed in Table IV, which are independent on the lattice constant and crystal structure. Then the total energy calculated by pair potentials could be compared with the *ab initio* calculations. Figure 2 shows that

TABLE III. Interionic pair potential parameters obtained in this work. The symbols + and - represent the cation and anion, respectively. The cutoff distance for short-range potential is 12.0 \AA.

Crystal	Ion pair	Function form	D (eV)	R (\AA)	γ
LiCl	++
	+-	Rep.-Exp.	1.3751	1.8750	5.9266
NaCl	--	Rep.-Exp.	0.4466	2.7929	8.7348
	++
	+-	Rep.-Exp.	0.2848	2.6499	8.6729
KCl	--	Morse	0.0244	3.7338	11.3902
	++
RbCl	+-	Rep.-Exp.	1.7149	2.3383	6.4557
	--	Morse	0.1177	3.7066	8.8093
RbCl	++	Rep.-Exp.	0.0572	2.6860	8.7701
	+-	Rep.-Exp.	0.5099	2.9085	8.2691
	--	Morse	0.0870	3.9386	7.8972

TABLE IV. The isolated-ion energy per ion E_{iso} between total energy and lattice energy.

ACl	LiCl	NaCl	KCl	RbCl
E_{iso} (eV/ion)	-297.45	-856.49	-593.97	-534.88

the present interionic potentials well reproduce the total energies for all of B1-, B2-, B3-, and P4/mmm ACl crystals. This indicates that the interionic pair potentials have been correctly inverted from the pseudopotential total energies by lattice inversion without the prior fixed potential function forms.

Besides, whatever method was used to obtain the potentials, one of the important tests for the final validation is to use the potentials to calculate the properties of other structures that were not involved in the potential derivation. Then the lattice energies as functions of crystal volume V/V_0 (V_0 is the equilibrium volume of B1-ACl) were calculated for ACl crystals in other four structures, respectively. The four trial structures are B4 (wurtzite-type), $L1_0$ (CuAu-type), $B8_1$ (NiAs-type) and litharge (PbO-type),²⁷ respectively, as shown in Fig. 3. Their calculated lattice energies are shown in Fig. 4. In terms of the isolated-ion energy in Table IV, the lattice energies were also calculated from pseudopotential total energies by the CASTEP code. Figure 4 shows the results via the present potentials are consistent with those from pseudopotential calculations. Although there is an obvious difference between the potential results and CASTEP calculation for litharge-type ACl, the overall agreement is satisfactory. This is mainly attributed to the fact that the present potentials were extracted from the four different structures, whose lattice constants range from 4.0 to 16.0 Å. Besides the phase space includes the configurations of four-, six-, and

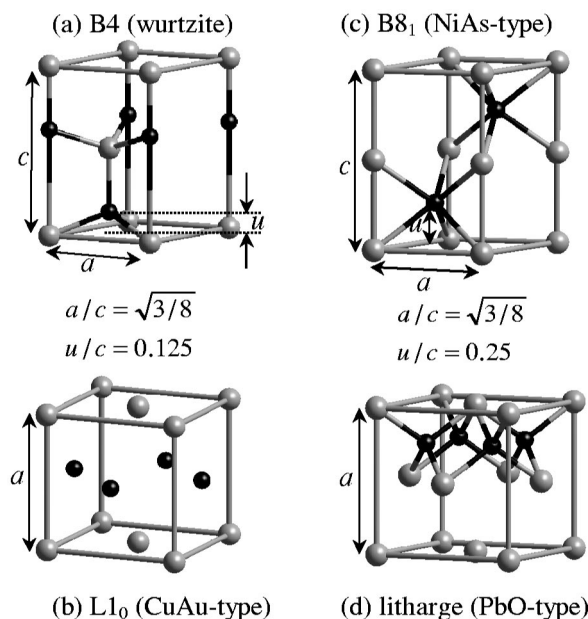


FIG. 3. The trial structures used to test the quality of interionic potentials. Phases B4 and $B8_1$ are both characterized by three parameters a , c , and u (distance of a layer of cations parallel to the basal plane from the underlying layer of anions).

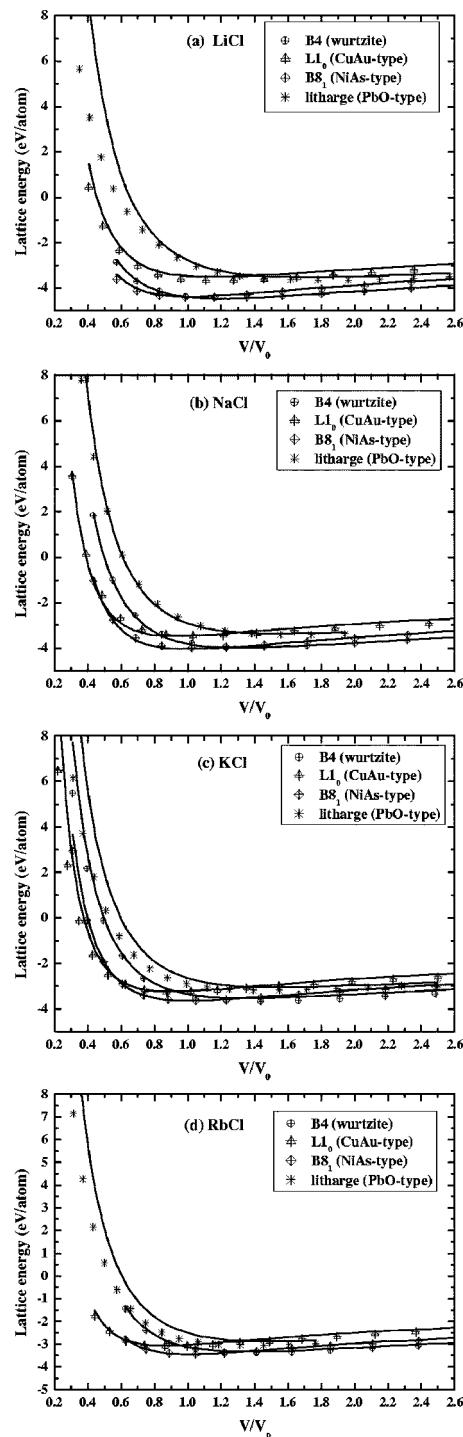


FIG. 4. Lattice energies versus the volume V/V_0 (V_0 is the equilibrium volume of B1-ACl) in trial structures. The scatter points were calculated by CASTEP code, and the solid lines were produced by present interionic pair potentials.

eight-fold coordination numbers. Therefore, the phase space for deriving the interionic potential was obviously extended; then the present pair potentials are more valid than those only from the properties of the equilibrium state of one phase. So the new interionic pair potentials could be regarded to be promising in predicting the new structures.

TABLE V. Lattice constants and elastic constants of ACl in the B1 phase. The values enclosed within parentheses are the experimental data. The errors are taken account in terms of the experimental values at 0 K.

ACl		Lattice constant a_0 (Å)	Volume V_0 (Å ³)	Lattice energy E_{latt} (kcal/mol)	Bulk modulus B (GPa)	Elastic constants (GPa)		
						C_{11}	C_{12}	C_{44}
LiCl	Calc.	5.112	33.40	204.3	36.06	47.72	30.24	30.24
	Expt.	(5.114) ^a	(33.44) ^a	(201.8) ^b	(35.4) ^a	(60.74) ^c (49.27) ^d	(22.70) ^c (23.10) ^d	(26.92) ^c (24.95) ^d
	Δ%	-0.04	-0.1	1.2	1.9	-21.4	33.2	12.3
NaCl	Calc.	5.602	43.95	188.6	29.01	59.14	13.94	13.94
	Expt.	(5.640) ^a	(44.85) ^a	(185.3) ^b	(28.5) ^a	(57.33) ^c	(11.23) ^c	(13.31) ^c
	Δ%	-0.7	-2.0	1.8	1.8	3.2	24.1	4.8
KCl	Calc.	6.266	61.51	169.7	19.12	43.45	6.96	6.96
	Expt.	(6.294) ^a	(62.33) ^a	(169.5) ^b	(20.2) ^a	(48.32) ^c	(5.40) ^c	(6.63) ^c
	Δ%	-0.4	-1.3	1.2	-5.3	-10.1	28.9	5.0
RbCl	Calc.	6.617	72.43	160.2	16.60	38.18	5.81	5.81
	Expt.	(6.582) ^a	(71.29) ^a	(159.3) ^{b*}	(18.5) ^a	(42.97) ^c (36.46) ^d	(6.49) ^c (6.47) ^d	(4.93) ^c (4.68) ^d
	Δ%	0.5	1.6	5.6	-10.3	-11.1	-10.5	17.8

^aExperimental data at 0 K (Ref. 1).

^bThe value at 0 K, and the value marked by * was measured at room temperature and not extrapolated to 0 K (Ref. 25).

^cEither an experimental measurement at 4.2 °K, or an extrapolation of literature values to 0 K (Refs. 2, 28).

^dThe values measured at 295 K (Ref. 28).

B. Equilibrium properties of B1-ACl

As most of the previous potentials, the present potentials were used to calculate the equilibrium lattice energy, lattice constant, bulk modulus, and elastic constants for B1-type ACl crystals. The results are listed in Table V. By comparison, it is found that the present potentials well reproduce the equilibrium lattice constant, volume, and lattice energy. The maximum error for the lattice constant is not more than 0.7% of the experimental data. The error for equilibrium volume is within the 2% of measured values. The maximum error for lattice energy occurs for RbCl since the room temperature value is used without the value extrapolated to 0 K. As for the static mechanical properties, the calculated values are close in agreement with the experimental data. The maximum discrepancy exists for elastic constants C_{12} and C_{44} . This first may be the pair potentials are used in this paper, so the Cauchy violation cannot be correctly described. In order to explain this difference, the many-body effect should be considered in further work based on the present pair potentials. The final reason is the experimental values at 0 K in Table V are extrapolated from the 4.2 K or room-temperature data.²⁸ Especially for the LiCl and RbCl, their 0 K elastic constants were extrapolated from room-temperature measurements, this might introduce some errors. To some extent, our calculated values are closer to the room-temperature data than that extrapolated to 0 K, as shown in Table V. Therefore, the overall agreement between the calculations and experimental results has been obtained in terms of the present interionic potentials.

C. Molecular dynamics simulations

In addition to the static properties, the test could also be performed by using the same interionic potentials in

molecular-dynamics simulations. Here we have performed the molecular dynamics simulations at constant pressure and temperature (NPT) with a $4 \times 4 \times 4$ B1-ACl supercell, containing 512 ions. The initial configuration was generated by arranging 256 cations and 256 anions on the equilibrium sites of the B1 lattice. For the NPT ensemble, the temperature and pressure were kept constant by using an extended system²⁹ with a thermostat and barostat relaxation time of 0.1 ps. The temperature range for the simulation is 300–800 K with a step of 50 K. For each temperature at 1 atm pressure, the calculations were performed for 30 000 steps with a time step of 1.5×10^{-15} s. The simulations for the initial 10 000 steps were used for stabilizing the system, and the data after 10 000 time steps were used to calculate the properties of our interest.

Based on the simulations from 300 to 800 K, the temperature dependence of volume for ACl can be first obtained, as shown in Fig. 5. Although it is obvious for LiCl that the melting temperature is underestimated to be about 750 K, lower than 878 K observed in the experiments,³⁰ the present calculations are found to be in good agreement with the experimental data³¹ and the previous calculations³² before the melting. For the RbCl crystal, the molecular-dynamics simulations give the close results, despite a little overestimation at a higher temperature. As for the NaCl and KCl, it can be seen in Fig. 5 that better results are given to be in good agreement with the experimental values.³³

The temperature dependence of the lattice constant can also be obtained from the molecular-dynamics simulations, then the bulk modulus B_T and elastic constant C_{ij} of ACl can also be calculated from the second derivatives of lattice energy at different temperatures. The results are shown in Fig. 6, in which the experimental data³⁴ and He's calculations³² are also included. By comparison for the bulk modulus, in

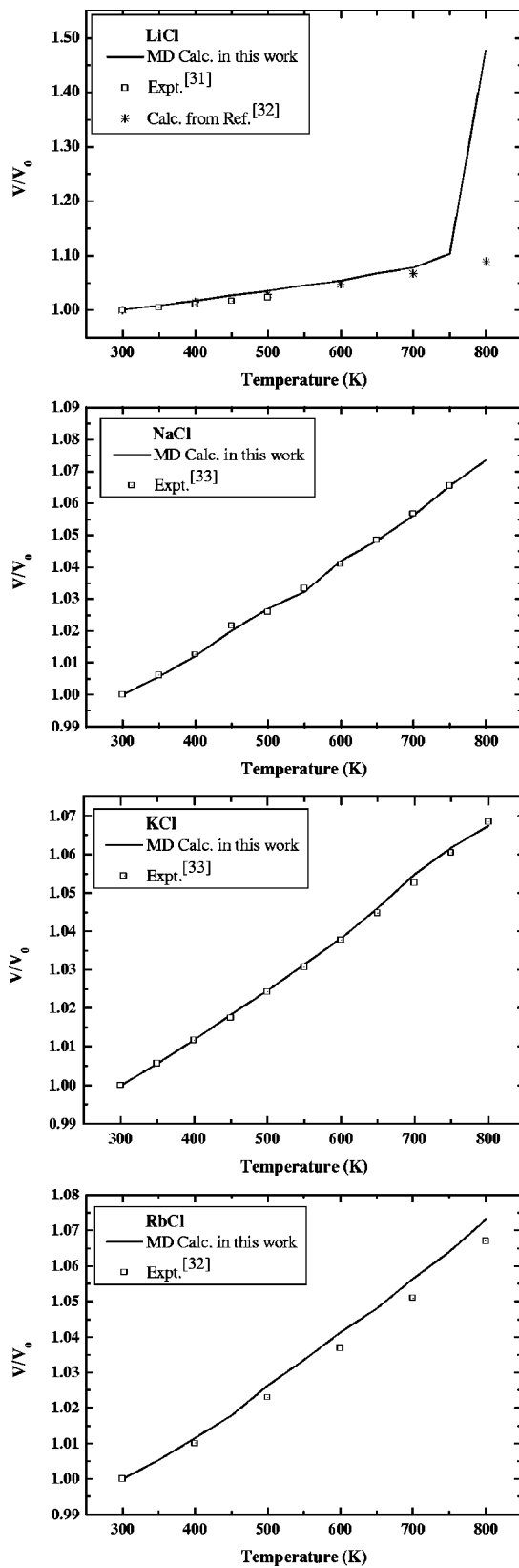


FIG. 5. The temperature dependence of volume for ACI in the range of 300–800 K.

spite of the overestimation for NaCl, it is found from 300–800 K that the calculated B_T is closer to the experiments than that of He *et al.*,³² especially for the LiCl. As for the elastic constants C_{ij} , the present calculations also give the good

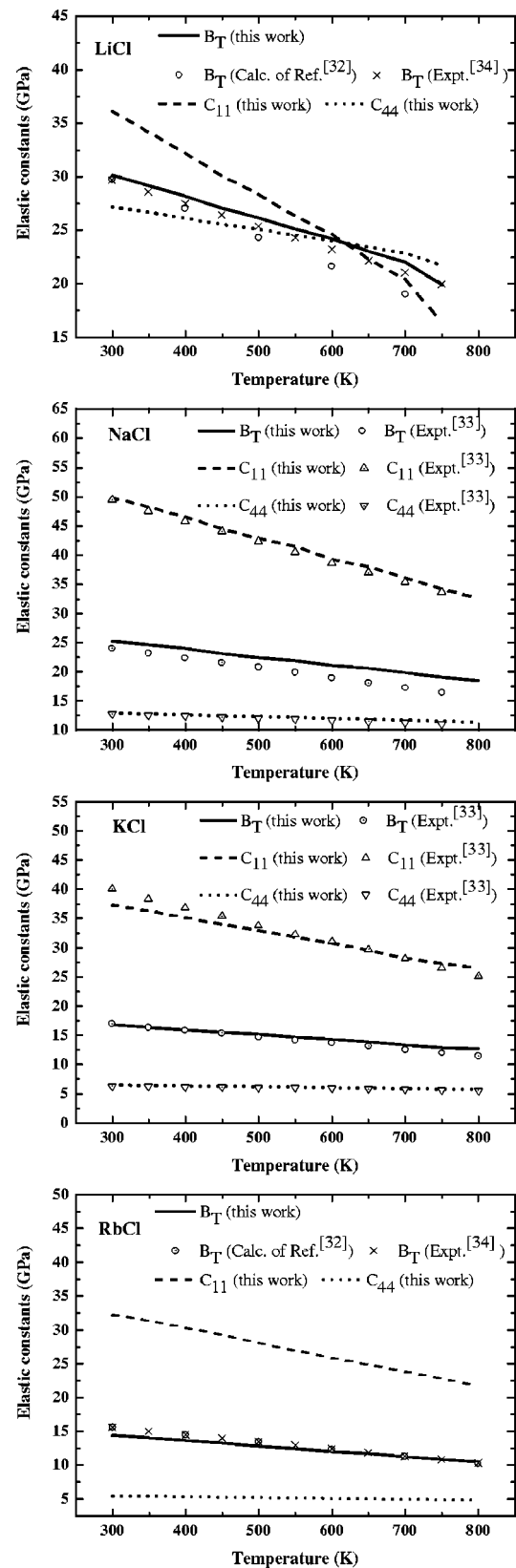


FIG. 6. The temperature dependences of bulk modulus and elastic constants from 300 to 800 K.

agreement with the experimental values³³ that are available. Since the temperature dependences of elastic constants are not available for LiCl and RbCl, the present calculations could be regarded as a prediction in the range of 300–800 K.

Despite the fact that there is the difference between the present calculations and experiments, it is clear that the present molecular-dynamics simulations give the overall agreement with the experimental data^{31,33,34} available. This indicates that the temperature dependences of volume, bulk modulus, and elastic constants have been well described by the lattice inversion pair potentials.

IV. DISCUSSIONS AND CONCLUSIONS

Based on the interionic potentials from lattice inversion, the equilibrium properties have been well reproduced to be in agreement with the experimental data, which are not involved in the derivation of potentials at all. Besides the temperature dependences of volume, bulk modulus, and elastic constants are also found to be in agreement with the experimental values and some previous calculations. This suggests that the present potentials are not only valid for a small part around the equilibrium position, but also can give encouraging results apart from the equilibrium position. Although the Cauchy violation in a rock salt structure has not been shown by the two-body potential model, the good transferability in eight phases has been obtained by the present pair potentials with simple function forms. This ability of a single set of potentials indicates that some many-body characters have been implicitly involved to cover different coordination numbers. Since the limit of pairwise potential form, we have to point out that some many-body properties may not be well described, such as the Cauchy violation. And for the defects, vacancies, and surfaces, the pair potentials could not give the satisfactory results because the structural local anisotropy deformation cannot be correctly described within the context of pair potentials. Therefore, the three-body potential forms should be introduced in future work. Nevertheless, since the present pair potentials are valid over a wide range of interionic spacings and coordination environments, we believe that the present potentials could be used to predict the structures of molten salt, alkali chloride clusters, and high-pressure-induced phase transition. In these cases, no special structure can be regarded as the most important, and the structures with different coordination numbers and interionic separations have to be considered, and then the present calculations suggest that this ability has been exhibited by the present interionic potential.

In summary, a new method for deriving the *ab initio* interionic potentials has been proposed and demonstrated through a series of alkali chlorides. According to our scheme, a series of *ab initio* total energy curves are calculated for several relevant structures with same stoichiometry. Then from the total energy difference, one can extract three partial lattice energy curves; each of them is only the sum of one kind of pair potential. Based on the Chen-Möbius lattice inversion, the three interionic pair potentials are derived one by one. In the above derivation, there is no need to select a prior potential function form and give empirical fixed charges on ions. The effective charges on ions can be determined by fitting to the total-energy difference between B1- and B3-ACl crystals at a larger lattice constant. And the appropriate function forms could be selected in terms of the final shape of potential curves. Since these new interionic

potentials are derived from *ab initio* calculations for ACl in several relevant structures, not only the properties of the used structures but also those of unused models have been well reproduced. This may be attributed to the wide range of pseudopotential total-energy calculations in different structures. Instead of only the configuration's nearby equilibrium state of rock-salt phase in conventional methods, the phase space for deriving the interionic potentials has been significantly extended to cover a larger range of interionic separations and coordination numbers. Therefore, these new interionic potentials may be promising in exploring and predicting the properties of ionic crystals in new phases. This indicates that this new method is worth further refinement and extending to other ionic crystals.

ACKNOWLEDGMENTS

This work was supported in part by the National Science Foundation of China, and in part by the National Advanced Materials Committee of China. Special thanks should be given to the support from the 973 Project in China (Grant No. G2000067101) and the National Nature Science Foundation of China (Grant No. 10274035).

- ¹A. J. Cohen and R. G. Gordon, *Phys. Rev. B* **12**, 3228 (1975).
- ²M. J. L. Sangster and M. Dixon, *Adv. Phys.* **25**, 247 (1976).
- ³C. R. A. Catlow, K. M. Diller, and M. J. Norgett, *J. Phys. C* **10**, 1395 (1977).
- ⁴H. Zhang and M. S. T. Buckowski, *Phys. Rev. B* **44**, 2495 (1991).
- ⁵J. M. Recio, E. Francisco, M. Flórez, and A. M. Pendás, *J. Phys.: Condens. Matter* **5**, 4975 (1993).
- ⁶A. M. Pendás, V. Lunaña, J. M. Recio, M. Flórez, E. Francisco, and M. A. Blanco, *Phys. Rev. B* **49**, 3066 (1994).
- ⁷M. Prencipe, A. Zupan, R. Dovesi, E. Aprà, and V. Saunders, *Phys. Rev. B* **51**, 3391 (1995).
- ⁸W. N. Mei, L. L. Boyer, M. J. Mehl, M. M. Ossowski, and H. T. Stokes, *Phys. Rev. B* **61**, 11425 (2000).
- ⁹R. Eggenhoffner, F. G. Fumi, and C. S. N. Murthy, *J. Phys. Chem. Solids* **43**, 583 (1982).
- ¹⁰J. Shanker and M. Kumar, *Phys. Status Solidi B* **142**, 325 (1987).
- ¹¹J. D. Gale, *Philos. Mag. B* **73**, 3 (1996).
- ¹²J. D. Gale, C. R. A. Catlow, and W. C. Mackrodt, *Modell. Simul. Mater. Sci. Eng.* **1**, 73 (1992).
- ¹³R. M. Fracchia, G. D. Barrera, N. L. Allan, T. H. K. Barron, and W. C. Mackrodt, *J. Phys. Chem. Solids* **59**, 435 (1998).
- ¹⁴M. Wilson and P. A. Madden, *Faraday Discuss.* **106**, 339 (1997).
- ¹⁵J. G. Rodeja, M. Meyer, and M. Hayoun, *Modell. Simul. Mater. Sci. Eng.* **9**, 81 (2001).
- ¹⁶A. E. Carlsson, C. D. Gelatt, and H. Ehrenreich, *Philos. Mag. A* **41**, 241 (1980).
- ¹⁷N.-X. Chen, Z.-D. Chen, and Y.-C. Wei, *Phys. Rev. E* **55**, R5 (1997).
- ¹⁸N.-X. Chen, X.-J. Ge, W.-Q. Zhang, and F.-W. Zhu, *Phys. Rev. B* **57**, 14203 (1998).
- ¹⁹N.-X. Chen, J. Shen, and X. Su, *J. Phys.: Condens. Matter* **13**, 2727 (2001).
- ²⁰N.-X. Chen and G.-B. Ren, *Phys. Rev. B* **45**, 8177 (1992).
- ²¹M. C. Payne, M. P. Teter, D. C. Allan, T. A. Arias, and J. D. Joannopoulos, *Rev. Mod. Phys.* **64**, 1045 (1992).
- ²²V. Milman, B. Winkler, J. A. White, C. J. Pickard, M. C. Payne, E. V. Akhmatkaya, and R. H. Nobes, *Int. J. Quantum Chem.* **77**, 895 (2000).
- ²³J. P. Perdew, J. A. Chevary, S. H. Vosko, K. A. Jackson, M. R. Pederson, D. J. Singh, and C. Fiolhais, *Phys. Rev. B* **46**, 6671 (1992).
- ²⁴H. J. Monkhorst and J. D. Pack, *Phys. Rev. B* **13**, 5188 (1976).
- ²⁵C. Kittel, *Introduction to Solid State Physics*, 7th ed. (Wiley, New York, 1996), pp. 66–73.
- ²⁶P. P. Ewald, *Ann. Phys. (N.Y.)* **64**, 253 (1921).
- ²⁷M. Wilson, P. A. Madden, S. A. Peebles, and P. W. Fowler, *Mol. Phys.* **88**, 1143 (1996).

- ²⁸J. T. Lewis, A. Lehoczy, and C. V. Briscoe, *Phys. Rev.* **161**, 877 (1967).
- ²⁹S. Melchionna, G. Ciccotti, and B. L. Hulan, *Mol. Phys.* **78**, 533 (1993).
- ³⁰D. B. Sirdeshmukh, L. Sirdeshmukh, and K. G. Subhadra, *Alkali Halides—A Handbook of Physical Properties*, Springer Series in Material Science (Springer, Berlin, 2001), p. 70.
- ³¹O. Madelung, *Landolt–Börnstein Numerical Data and Functional Relationships in Science and Technology (F, Cl, Br, I (VIIth Main Group). Halides and Complex Halides)*, Springer 1.2.1, 1982, p. 343.
- ³²Q. He and Z.-T. Yan, *Phys. Status Solidi B* **223**, 767 (2001).
- ³³A. Vijay and T. S. Verma, *Physica B* **291**, 373 (2000).
- ³⁴R. S. Carmichael, *CRC Handbook of Physical Properties of Rocks* (CRC, Boca Raton, FL, 1984), Vol. VIII, pp. 60–69.